

Ferroptosis Induction and Cisplatin Chemoresistance Reversal by MASTL Inhibition in Ovarian Cancer

Rong Yan, Yanting Gu*

Shenyang Pharmaceutical University, Shenyang, China

Keywords: Ovarian Cancer, MASTL, Cisplatin Resistance, Ferroptosis

Abstract: Ovarian cancer remains the leading cause of mortality among gynecologic malignancies, posing a significant threat to women's health worldwide. Although cytoreductive surgery combined with platinum-based chemotherapy constitutes the standard treatment for epithelial ovarian cancer, therapeutic efficacy is markedly limited in patients with platinum-resistant recurrent disease. Microtubule-associated serine/threonine kinase-like (MASTL), a key regulator of mitotic progression, has recently garnered increasing attention due to its association with poor prognosis and chemotherapy resistance in various cancers. However, the precise role of MASTL deregulation in ovarian cancer progression and chemoresistance remains poorly understood. In this study, in vitro experiments demonstrated that MASTL is aberrantly overexpressed in ovarian cancer cells, particularly in cisplatin-resistant cell lines (CoC1/DDP). Genetic silencing of MASTL significantly sensitized resistant cells to cisplatin, induced apoptosis, and enhanced chemotherapy-induced cell death, potentially through the modulation of ferroptosis-related pathways. Further, treatment with a small-molecule MASTL inhibitor potentiated cisplatin-induced DNA damage and apoptosis in vitro. To our knowledge, this is the first study to demonstrate that pharmacological inhibition of MASTL enhances cisplatin sensitivity in ovarian cancer by ferroptosis. These findings suggest a promising therapeutic strategy targeting MASTL to overcome chemoresistance and improve clinical outcomes in patients with ovarian cancer.

1. Introduction

Ovarian cancer is one of the most prevalent malignant tumors of the female reproductive system. Characterized by rapid progression and early metastatic spread, ovarian cancer is associated with poor patient survival outcomes. Although cytoreductive surgery remains a cornerstone of treatment, chemotherapy continues to serve as the primary therapeutic modality for epithelial ovarian cancer, particularly in both adjuvant and recurrent settings. However, the therapeutic efficacy of chemotherapy is markedly diminished in cases of platinum-resistant recurrence [1]. Consequently, overcoming intrinsic or acquired chemoresistance in tumor cells remains a major challenge in the treatment of ovarian cancer.

Dysregulated mitosis is a hallmark of cancer progression, and mitotic kinases and cell cycle checkpoint regulators offer promising opportunities for selective anticancer therapies. Among these, microtubule-associated serine/threonine kinase-like (MASTL) has garnered considerable attention in recent years as a critical regulator of mitotic progression [2]. MASTL mediates phosphorylation of

α -endosulfine (ENSA) and/or cAMP-regulated phosphoprotein 19 (ARPP19), leading to inhibition of the phosphatase activity of PP2A/B55, a form of protein phosphatase 2A that contains a B55-family regulatory subunit. PP2A is a ubiquitously expressed serine/threonine phosphatase that regulates numerous cellular functions through dephosphorylation of key signaling proteins, including Akt, p53, c-Myc, and β -catenin [3]. MASTL overexpression has been reported in multiple tumor types, including breast cancer, head and neck squamous cell carcinoma (HNSCC), and ovarian cancer, where its high expression is significantly correlated with aggressive clinicopathological features, poor prognosis, and resistance to platinum-based chemotherapy [4]. Aberrant MASTL activity has been implicated in oncogenic transformation, contributing to chromosomal instability and dysregulation of essential oncogenic signaling pathways. Notably, Aimin Peng and colleagues demonstrated that in HNSCC, MASTL upregulation impairs the DNA damage response, inhibits apoptosis, and promotes tumor cell survival under cisplatin treatment in an ENSA-dependent manner [5]. Collectively, these findings position MASTL as a novel therapeutic target in cancer treatment [6]. Besides, Ferroptosis is a newly identified form of iron-dependent regulated cell death that is characterized by the accumulation of lipid peroxides. Unlike traditional cell death processes, such as apoptosis, necrosis, or autophagy, ferroptosis exhibits unique morphological and molecular features, positioning it as an emerging therapeutic target in cancer treatment [7].

Building on these insights, this study further explored the role of MASTL deregulation in ovarian cancer progression and chemoresistance. Notably, it was found that treatment with the MASTL inhibitor MKI-1, in combination with cisplatin, significantly suppressed tumor growth in vitro. These findings highlight a promising therapeutic strategy to overcome drug resistance by exploiting MASTL as a novel molecular target.

2. Materials and Methods

2.1. Cell culture

The ovarian cancer cell lines CoC1 and CoC1/DDP were obtained from the China Center for Type Culture Collection, while the A2780 ovarian cancer cell line and the immortalized normal ovarian epithelial cell line (HOSEC) were purchased from Hunan Fenghui Biotechnology Co., Ltd (Hunan, China).

HOSEC cells were cultured in Dulbecco's Modified Eagle Medium (DMEM) supplemented with 10% fetal bovine serum (FBS) and 1% penicillin–streptomycin. CoC1 and A2780 cells were maintained in RPMI-1640 medium supplemented with 10% FBS and 1% penicillin–streptomycin. The cisplatin-resistant CoC1/DDP cells were cultured in RPMI-1640 medium containing 10% FBS, 1% penicillin–streptomycin, and 2 μ M cisplatin (DDP; MedChemExpress, USA). All of the cells were maintained in a humidified incubator at 37 °C with 5% CO₂.

2.2. RNA interference

Small interfering RNAs (siRNAs) targeting MASTL were used to achieve MASTL knockdown, with a non-targeting siRNA serving as a negative control. A panel of MASTL-targeting siRNAs was obtained from GenePharma (Shanghai, China). Cells were seeded in 6-well plates and transiently transfected with siRNAs at a final concentration of 1.5 μ M using siRNA-Mate Plus transfection reagent (GenePharma), according to the manufacturer's instructions. At 48 hours after transfection, cells were harvested for mRNA and protein expression analysis via quantitative real-time PCR (qPCR) and Western blotting. Of the four siRNA constructs tested, siMASTL-3 (sense: 5'-AAGGUUACCCAUGCAGUUGTT-3'; antisense: 5'-CAACUGCAUGGGUAACCUUTT-3') exhibited the highest knockdown efficiency, and it was selected for subsequent experiments.

After 48 hours of transfection, cells were subjected to downstream assays, including cell proliferation analysis using the CCK-8 assay, apoptosis detection by flow cytometry, and pathway-related experiments involving cisplatin (DDP) treatment.

2.3. Real-time PCR

Total RNA was isolated from RNA-interfered cells using Triquick Reagent (Trizol Substitute, Solarbio, China), in accordance with the manufacturer's instructions. RNA was reverse transcribed to cDNA using the EasyScript One-Step gDNA Removal and cDNA Synthesis SuperMix (TRANSGEN Biotech, AE311). All of the qPCR reactions were performed in 20 μ L volumes using 2 \times Q3 SYBR qPCR Master Mix (Universal) (22204, TOLOBIO) and amplified on a SLAN-96H Real-Time PCR Instrument (Shanghai Hongshi Medical Technology Co., Ltd., China).

All of the primers were synthesized by Shanghai Generay Biotechnology. The primers for MASTL were as follows: forward primer, 5'-CGCTCTTGTGTAAACCTTGC-3'; reverse primer, 5'-AGCCCACTGATTTGACTGATG-3'. The primers for GAPDH were: forward primer, 5'-AATCCCATCACCATCTTC-3'; reverse primer, 5'-AGGCTGTTGTCATACTTC-3'. The PCR assay parameters were set as follows: initial denaturation at 95 $^{\circ}$ C for 5 minutes, followed by 40 cycles of denaturation at 95 $^{\circ}$ C for 10 seconds, and annealing/extension at 60 $^{\circ}$ C for 30 seconds. Comparative quantification was conducted using the $2^{-\Delta\Delta C_t}$ method, with glyceraldehyde-3-phosphate dehydrogenase (GAPDH) serving as the endogenous control.

2.4. Western blotting

Cultured cells and tumor tissues were lysed in extraction buffer. Equal amounts of protein from each sample were separated by sodium dodecyl sulfate-polyacrylamide gel electrophoresis (SDS-PAGE), transferred to polyvinylidene fluoride membranes, and blocked with 5% bovine serum albumin. Membranes were incubated overnight at 4 $^{\circ}$ C with primary antibodies against MASTL (Absin, Shanghai, China), GPX4 (Abcam, USA), SLC7A11 (Abcam, USA), DMT1 (Proteintech, UK), P53 (Proteintech, UK), and GAPDH (Proteintech, UK). After washing, membranes were incubated with horseradish peroxidase (HRP)-conjugated secondary antibodies (ZSGB-Bio, China). Protein bands were visualized using an enhanced chemiluminescent HRP substrate (Life-iLab Biotech, Shanghai, China), and relative band intensities were quantified using a gel imaging analysis system (Tanon, China).

2.5. CCK-8 assay

CoC1/DDP-siNC and CoC1/DDP-siMASTL cells were seeded into 96-well plates and treated with various concentrations (0, 5, 10, 20, 40, 80, and 160 μ M) of cisplatin (DDP; MedChemExpress, USA) for 24 hours, followed by analysis using a Cell Counting Kit-8 (CCK-8). The 50% inhibitory concentration (IC₅₀) of DDP was determined based on the relative survival curve. The CCK-8 assay was used to assess DDP resistance.

CoC1/DDP cells were seeded into 96-well plates and treated with a range of concentrations (0, 1, 2, 5, 10, 25, 50, and 100 μ M) of GKI-1 (MedChemExpress, USA) for 24 hours, followed by CCK-8 analysis. The inhibition rate was calculated using the following formula: $(1 - (\text{Absorbance of treated sample} - \text{blank}) / (\text{Absorbance of control} - \text{blank})) \times 100\%$.

To assess the type of cell death induced by DDP following MASTL siRNA knockdown, CCK-8 assays were performed with four cell death inhibitors: ferrostatin-1 (Fer-1), tetrathiomolybdate (TTM), Z-VAD-FMK, and necrostatin-1 (Nec-1). Fer-1, Z-VAD-FMK, and Nec-1 were obtained from MedChemExpress (USA), and TTM was purchased from Selleckchem (USA). CoC1/DDP cells

were cultured in 6-well plates and transiently transfected with MASTL siRNA for 48 hours. Cells were then treated with Fer-1 (20 μ M), TTM (10 μ M), Z-VAD-FMK (5 μ M), or Nec-1 (2 μ M) for 2 hours, followed by the addition of DDP at a final concentration of 20 μ M for 24 hours.

Cell viability was subsequently evaluated using the CCK-8 assay (Cat# C0039, Beyotime, Shanghai, China) according to the manufacturer's instructions. Absorbance was measured at 450 nm, and wells without cells served as blanks.

2.6. Immunofluorescence assay for DNA damage

Cells were seeded in 6-well plates and subjected to different experimental treatments as specified. DNA damage in ovarian cancer cells was assessed using the DNA Damage Assay Kit with γ H2AX immunofluorescence (C2035, Beyotime, China), following the manufacturer's instructions. After treatment, cells were fixed, permeabilized, and incubated sequentially with a γ H2AX primary antibody and a fluorescently labeled secondary antibody. Fluorescence signals were visualized and captured using a fluorescence microscope system (ECLIPSE Ni Series, Nikon, Japan).

2.7. Apoptosis assay

Apoptosis was analyzed using the Annexin V-FITC/PI Apoptosis Detection Kit (Beyotime, China). Cells were harvested, washed with cold phosphate-buffered saline (PBS), and resuspended in binding buffer. Annexin V-FITC and propidium iodide (PI) were added according to the manufacturer's instructions. After incubation in the dark, the samples were examined on a CytoFLEX flow cytometer (Beckman Coulter, USA). Data were analyzed using CytExpert software (Beckman Coulter, USA) to distinguish viable, apoptotic, and necrotic cells. The proportion of apoptotic cells was calculated for each group, and all of the experiments were performed in triplicate.

2.8. Statistical analysis

GraphPad Prism version 8.4.3 (USA) was used for data analysis and visualization. All of the results are expressed as mean \pm standard deviation (SD). Group comparisons were performed using one-way or two-way analysis of variance (ANOVA), followed by Tukey's multiple comparisons test. Statistical significance was defined as follows: * $P < 0.05$, ** $P < 0.01$, *** $P < 0.001$, and **** $P < 0.0001$; "ns" indicates no significant difference.

3. Results

3.1. MASTL is highly expressed in ovarian cancer cells, and silencing MASTL induces apoptosis

Recent studies have highlighted the pivotal regulatory role of MASTL in tumor development and progression [6]. Prior research has shown that MASTL overexpression significantly enhances the invasive and migratory capabilities of breast and colorectal cancer cell lines [8]. To assess the expression profile of MASTL in ovarian cancer, particularly in platinum-resistant subtypes, we performed Western blot and qRT-PCR analyses across a panel of cell lines, including human normal ovarian surface epithelial cells (HOSECs), the cisplatin-resistant ovarian cancer cell line CoC1/DDP, its parental CoC1 line, and the A2780 ovarian cancer cell line.

Our results revealed that both MASTL protein and mRNA levels were significantly upregulated in ovarian cancer cells (A2780, CoC1, and CoC1/DDP) compared to HOSECs ($P < 0.05$). Notably, the highest expression was observed in the cisplatin-resistant CoC1/DDP cells (Figure 1A–C).

To explore the functional role of MASTL, we generated MASTL-silenced CoC1/DDP cells using

small interfering RNA (siRNA). Knockdown efficiency was confirmed by qRT-PCR and Western blot, which demonstrated that siMASTL-3 was the most effective of the tested siRNA constructs, and it was selected for subsequent experiments.

MASTL knockdown was achieved by transfecting CoC1/DDP cells with siMASTL-3 or a negative control siRNA (siNC), followed by 48 hours of incubation. Cells were then treated with various concentrations of cisplatin, and cell viability was assessed using the CCK-8 assay. The results indicated that MASTL silencing significantly enhanced the sensitivity of CoC1/DDP cells to cisplatin and promoted apoptosis (Figure 1D). To further validate this observation, flow cytometry was used to quantify apoptosis. Compared with the Vehicle + siNC group, apoptosis rates were markedly elevated in the Vehicle + siMASTL-3, siNC + DDP, and especially in the siMASTL + DDP groups ($P < 0.001$) (Figure 1E,F). Among these groups, the combination of siMASTL and cisplatin yielded the highest level of apoptosis, suggesting a synergistic interaction. These findings indicate that MASTL knockdown potentiates cisplatin-induced apoptosis and enhances the chemosensitivity of cisplatin-resistant ovarian cancer cells.

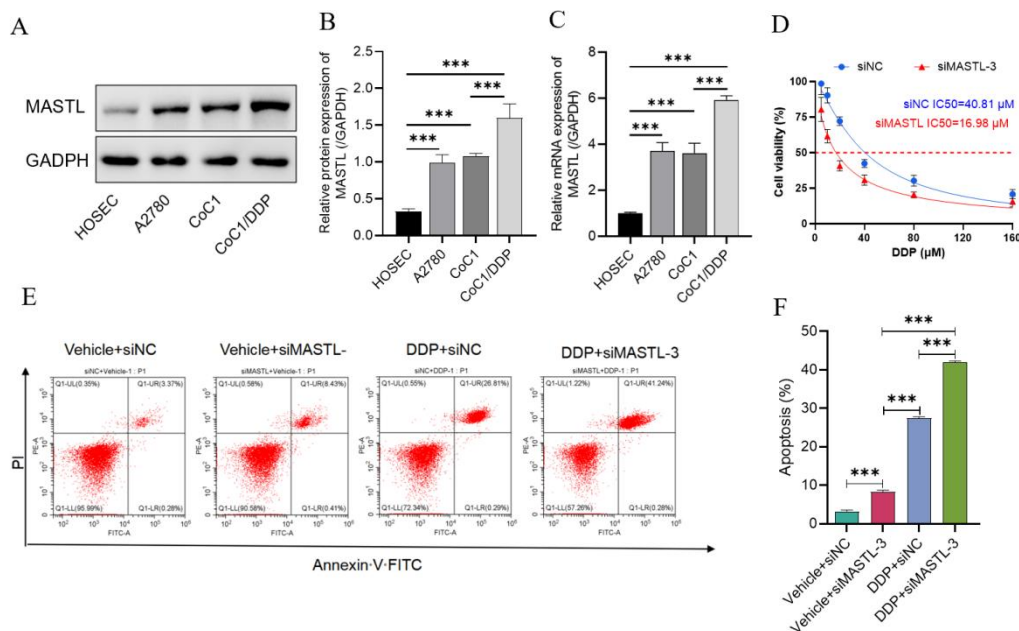


Figure 1: MASTL is highly expressed in ovarian cancer cells, and silencing MASTL induces apoptosis

* $P < 0.05$, ** $P < 0.01$, *** $P < 0.001$, ns, no significance.

(A-B) MASTL Western blot analysis. The protein expression of MASTL was analyzed between human ovarian cancer cells A2780, CoC1, CoC1 DDP, and human normal ovarian epithelial cells (HOSEC). (C) MASTL mRNA analysis by RT-PCR. mRNA level of MASTL was analyzed between human ovarian cancer cells A2780, CoC1, CoC1 DDP, and human normal ovarian epithelial cells (HOSEC). (D) Cisplatin resistance analysis using IC50 concentrations. The effect of MASTL silencing on sensitivity to cisplatin (DDP) was analyzed. The experiment was divided into the following groups: siNC group with a series of DDP and siMASTL group with a series of DDP. (E-F) Construction of MASTL siRNA and siNC transfection into CoC1/DDP cells for 48 hours. CoC1/DDP cells treated with siNC and siMASTL were incubated at 37°C for 24 hours with DDP (20 μmol/L). Apoptosis levels were detected by flow cytometry. The experiment was divided into the following groups: Vehicle + siNC group; Vehicle + siMASTL-3 group; DPP+ siNC group; and DDP+siMASTL group.

3.2. MASTL kinase inhibitors (GKI-1 and MKI-1) increase cisplatin sensitivity, promote DNA damage, and accelerate apoptosis in resistant cells

Ocasio et al. first identified GKI-1 as a small-molecule inhibitor of MASTL, selected for its ability to reduce phosphorylation of ENSA [9]. As the first reported MASTL kinase inhibitor, GKI-1 has drawn considerable interest due to its potential antitumor properties. Although GKI-1 demonstrates some off-target effects, Aimin Peng et al. reported that it significantly suppressed proliferation of oral squamous cell carcinoma cell lines (UMSCC-38), particularly in combination with cisplatin [5]. This co-treatment produced a synergistic antitumor effect and markedly reduced cell viability. Notably, GKI-1 acts in a dose-dependent manner: at high concentrations (50 μ M), it induces mitotic arrest, whereas at lower concentrations (10 μ M), it enhances cisplatin sensitivity without fully disrupting mitosis. Given that MASTL kinase activity is reduced during interphase, the sensitizing effect of low-dose GKI-1 may offer a more feasible and clinically translatable therapeutic approach. To explore the potential of GKI-1 in modulating cisplatin resistance in ovarian cancer, we evaluated its impact on CoC1/DDP cell viability using the CCK-8 assay. GKI-1 significantly inhibited the proliferation of CoC1/DDP cells in a dose-dependent manner (Figure 2A).

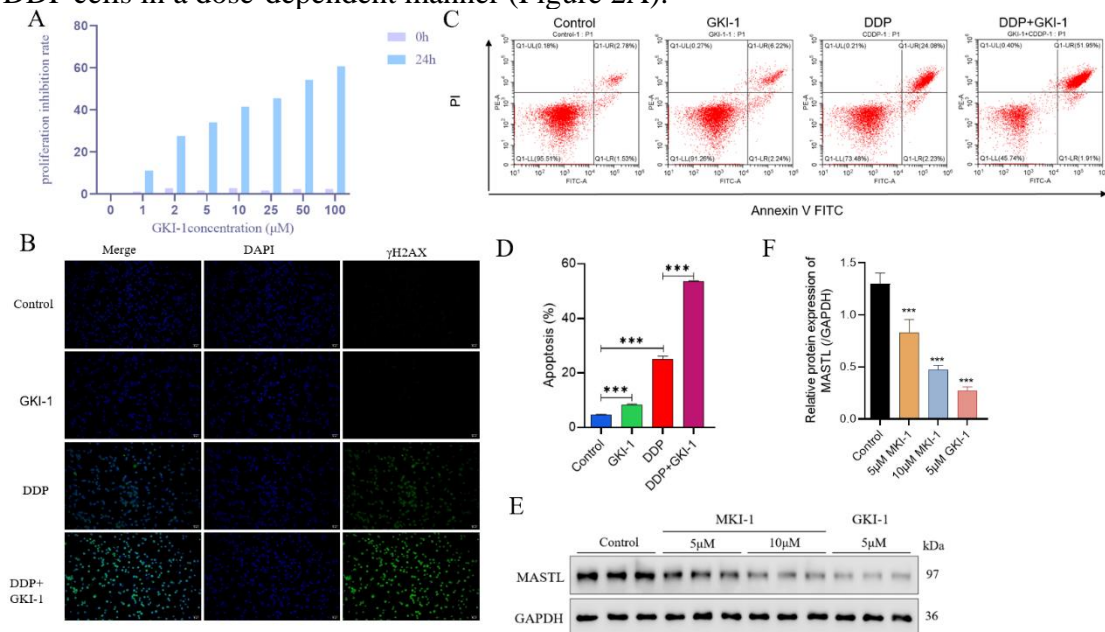


Figure 2: Small-Molecule MASTL Kinase Inhibitor Increases Cisplatin Sensitivity, Promotes DNA Damage, and Enhances Apoptosis in Cisplatin-Resistant Cells.

* $P < 0.05$, ** $P < 0.01$, *** $P < 0.001$, ns, no significance.

(A) CoC1/DDP cells were cultured with a series of GKI-1 concentrations. Cell viability was assessed using the CCK-8 assay to determine the effect of GKI-1 on the cisplatin resistance of CoC1/DDP cells. (B) Cells were plated at 5×10^5 cells/well in six-well plates, with three replicates per group. Following 24 hours of treatment with GKI-1 and DDP, DNA damage was detected by γ H2AX staining. Control group: Control - CoC1/DDP cells; GKI group: CoC1/DDP cells + GKI-1 (5 μ M); DDP group: CoC1/DDP cells + DDP (20 μ M); DDP+GKI group: CoC1/DDP cells + GKI-1 (5 μ M) + DDP (20 μ M). (C-D) As cell treatment in (B), after 24 hours of treatment, apoptosis was analyzed by flow cytometry. (E-F) CoC1/DDP cells were treated with GKI-1 (5 μ M), MKI-1 (5 μ M, 10 μ M) for 24 hours. Western blotting was used to detect MASTL protein levels.

Further building on Peng's findings, which showed that MASTL knockdown under cisplatin treatment (5 μ M) increased expression of the DNA damage marker γ -H2AX and activated DNA

damage response pathways (e.g., CHK2 phosphorylation and upregulation of cleaved caspase-3 and cleaved PARP1), we examined the effect of GKI-1 in combination with cisplatin in ovarian cancer cells. CoC1/DDP cells were treated with 5 μ M GKI-1 and 20 μ M cisplatin for 24 hours [5]. Immunofluorescence staining of γ -H2AX showed that the combination therapy markedly enhanced DNA damage in cisplatin-resistant cells (Figure 2B). Flow cytometric analysis confirmed that the combined treatment significantly increased apoptosis rates in CoC1/DDP cells compared to either agent alone (Figure 2C, D). These results suggest that GKI-1 potentiates cisplatin-induced cytotoxicity by promoting DNA damage and apoptosis, offering a promising strategy to overcome platinum resistance.

Jae-Sung Kim et al. identified a novel MASTL inhibitor, MKI-1, through virtual screening and in vitro kinase assays based on ENSA phosphorylation detection [4]. Molecular docking studies revealed that MKI-1 interacts specifically with the L113 residue within the MASTL kinase domain via hydrogen bonding, facilitating selective binding to the catalytic pocket. Mechanistically, MKI-1 activates PP2A phosphatase activity, leading to destabilization of the oncogenic protein c-Myc, and exerts both antitumor and radiosensitizing effects in breast cancer models. In vitro studies demonstrated potent anticancer activity and minimal toxicity, suggesting significant clinical potential. Additional in vitro kinase assays using the ADP-Glo system confirmed that MKI-1 inhibits MASTL kinase activity in a dose-dependent manner, with an IC_{50} comparable to GKI-1. MKI-1 significantly impaired malignant cell behavior in breast cancer while sparing normal mammary epithelial cells, supporting its therapeutic selectivity.

To assess the effects of MKI-1 and GKI-1 on MASTL protein expression, CoC1/DDP cells were treated with MKI-1 at concentrations of 5 μ M and 10 μ M for 24 hours. Western blot analysis showed that both MKI-1 and GKI-1 significantly reduced MASTL protein levels (Figure 2E, F). However, the precise molecular mechanisms by which these inhibitors downregulate MASTL remain to be elucidated.

3.3. MASTL gene silencing enhances cell death by ferroptosis

To further elucidate the molecular mechanisms by which MASTL gene silencing inhibits cell proliferation, we evaluated the impact of pathway-specific inhibitors. CoC1/DDP cells transfected with siMASTL were separately treated with Fer-1, TTM, and Z-VAD-FMK (an apoptosis inhibitor), and Nec-1, followed by cisplatin exposure. The ability of these inhibitors to reverse the effects of MASTL silencing would suggest the involvement of the corresponding pathways in the observed phenotype.

In this experiment, 5×10^5 cisplatin-resistant CoC1/DDP cells were seeded into 6-well plates and transfected with either siNC or siMASTL for 48 hours. Cells were then pretreated with the designated inhibitors for 2 hours and subsequently co-treated with cisplatin (20 μ M) and the corresponding inhibitors for 24 hours. Cell viability was assessed via the CCK-8 assay. Comparison between the siMASTL group and the siNC control group showed that Fer-1 and Nec-1 partially alleviated the inhibitory effect of MASTL knockdown on cell proliferation. These results indicate that ferroptotic and necroptotic pathways may contribute to the enhanced chemosensitivity observed in MASTL-silenced cells (Figure 3).

Recent studies have demonstrated that ferroptosis plays a key role in the regulation of ovarian cancer growth, with mechanisms involving the transsulfuration pathway, Hippo signaling, and the p53 pathway [7]. Uppada et al. reported that MASTL promotes tumor progression and chemoresistance in colon cancer via the Wnt/ β -catenin signaling pathway, regulating the phosphorylation of glycogen synthase kinase-3 beta (GSK3 β) [10]. Additionally, Chih-Hsiung Hsieh et al. showed that zero-valent iron nanoparticles induce ferroptotic cell death in lung cancer through

NRF2 degradation, mediated by the GSK3 β -TrCP axis via AMPK/mTOR pathway activation [11]. These findings collectively suggest that MASTL may influence ferroptosis sensitivity and, in doing so, regulate tumor cell survival and proliferation. The molecular mechanisms by which MASTL regulates ferroptosis and its broader impact on ovarian cancer progression need to be further investigated.

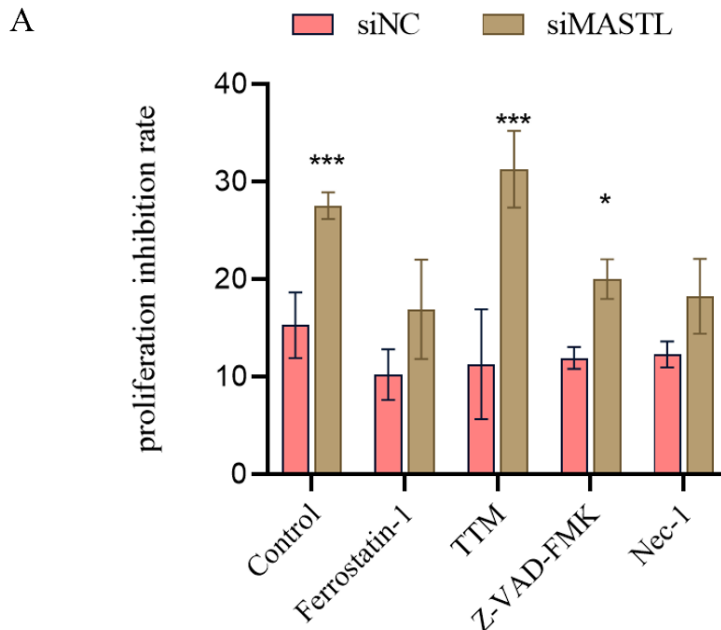


Figure 3: MASTL Gene Silencing Enhances Cell Death by Promoting Ferroptosis Sensitivity to Inhibit Tumor Cell Proliferation.

* $P < 0.05$, ** $P < 0.01$, *** $P < 0.001$, ns, no significance.

(A) Cells were transfected with SiNC and siMASTL for 48 hours. After this, the corresponding inhibitors were added for 2 hours of pretreatment, and the medium was replaced with one containing cisplatin (20 μ M) and inhibitors for 24 hours of intervention. Cell viability was detected by CCK8 assays. The experiment was divided into the following five groups: Control: DDP 20 μ M; Ferrostatin-1: DDP 20 μ M + Ferroptosis Inhibitor Ferrostatin-1 20 μ M; TTM: DDP 20 μ M + Copper-induced Cell Death Inhibitor Tetrathiomolybdate (TTM) 10 μ M; Z-VAD-FMK: DDP 20 μ M + Apoptosis Inhibitor Z-VAD-FMK 5 μ M; and Nec-1: DDP 20 μ M + Necrosis Inhibitor Nec-1 2 μ M.

4. Discussion

MASTL is a serine/threonine kinase that plays a critical role during the mitotic phase of the cell cycle. In recent years, it has gained significant attention for its function in inhibiting key cellular phosphatases during mitosis [3]. Specifically, MASTL regulates the activity of the PP2A-B55 complex by phosphorylating and activating its endogenous inhibitors, thereby promoting mitotic progression and establishing a novel regulatory mechanism for kinase-phosphatase interactions in cell cycle control. Interestingly, emerging evidence has linked the PP2A-B55 complex to the regulation of ferroptosis. Bo Qian et al. reported that the PP2A-B55 β complex mediates the dephosphorylation of phosphorylated GPX4 (p-GPX4) via retrograde p53 signaling. This PP2A-B55 β /p-GPX4Ser2/p53 axis represents a newly identified regulatory pathway involved in sorafenib-induced ferroptosis in liver cancer [12].

Based on these findings, we hypothesized that MASTL may modulate ferroptosis in ovarian cancer

by indirectly regulating the p53 signaling pathway, thereby affecting cisplatin sensitivity and tumor progression. To explore this hypothesis, we examined MASTL expression in drug-resistant ovarian cancer cell lines (CoC1/DDP), parental cancer cell lines (CoC1 and A2780), and normal ovarian epithelial cells. qRT-PCR and Western blot analyses confirmed that MASTL expression was significantly upregulated in ovarian cancer cells, particularly in the drug-resistant CoC1/DDP line. Functional assays demonstrated that MASTL knockdown markedly enhanced cisplatin sensitivity and significantly induced apoptosis in CoC1/DDP cells. Moreover, treatment with the small-molecule MASTL inhibitor GKI-1, in combination with cisplatin, further amplified DNA damage and apoptosis. Importantly, this effect was attenuated by the ferroptosis inhibitor Fer-1 and the necroptosis inhibitor Nec-1, suggesting that MASTL may promote tumor cell survival by suppressing ferroptosis. The mechanism need to be further investigated.

In summary, our findings suggest that MASTL inhibition not only suppresses ovarian tumor growth but also enhances ferroptosis, contributing to increased sensitivity to cisplatin. MASTL inhibitors exhibited significant antitumor effects, highlighting their potential as promising therapeutic agents for ovarian cancer. Given the pivotal role of MASTL in modulating the response of ovarian cancer cells to chemotherapeutic agents, targeting MASTL represents a compelling strategy to overcome drug resistance and enhance treatment efficacy. Despite these encouraging results, several challenges remain. Further studies are warranted to fully elucidate the molecular mechanisms underlying MASTL-mediated chemoresistance and to assess the clinical feasibility of MASTL inhibitors in ovarian cancer patients. Continued investigation in this area may ultimately lead to more effective therapeutic strategies and improved outcomes, offering new hope for patients facing this aggressive malignancy.

5. Conclusion

Altogether, the results indicate that deregulation of the MASTL gene significantly influences cisplatin sensitivity in ovarian cancer cells. While these findings highlight the therapeutic potential of combining MASTL inhibitors with cisplatin, further research is required to facilitate clinical translation and optimize therapeutic efficacy.

References

- [1] Morand, S., Devanaboyina, M., Staats, H., Stanbery, L., Nemunaitis, J.: Ovarian Cancer Immunotherapy and Personalized Medicine. *Int J Mol Sci.* 22, 6532 (2021). <https://doi.org/10.3390/ijms22126532>
- [2] Mochida, S., Maslen, S.L., Skehel, M., Hunt, T.: Greatwall phosphorylates an inhibitor of protein phosphatase 2A that is essential for mitosis. *Science.* 330, 1670–1673 (2010). <https://doi.org/10.1126/science.1195689>
- [3] Gharbi-Ayachi, A., Labbé J.-C., Burgess, A., Vigneron, S., Strub, J.-M., Brioudes, E., Van-Dorselaer, A., Castro, A., Lorca, T.: The substrate of Greatwall kinase, Arpp19, controls mitosis by inhibiting protein phosphatase 2A. *Science.* 330, 1673–1677 (2010). <https://doi.org/10.1126/science.1197048>
- [4] Kim, A.-Y., Yoon, Y.N., Leem, J., Lee, J.-Y., Jung, K.-Y., Kang, M., Ahn, J., Hwang, S.-G., Oh, J.S., Kim, J.-S.: MKI-1, a Novel Small-Molecule Inhibitor of MASTL, Exerts Antitumor and Radiosensitizer Activities Through PP2A Activation in Breast Cancer. *Front. Oncol.* 10, (2020). <https://doi.org/10.3389/fonc.2020.571601>
- [5] Gouttia, O.G., Zhao, J., Li, Y., Zwiener, M.J., Wang, L., Oakley, G.G., Peng, A.: The MASTL-ENSA-PP2A/B55 axis modulates cisplatin resistance in oral squamous cell carcinoma. *Front Cell Dev Biol.* 10, 904719 (2022). <https://doi.org/10.3389/fcell.2022.904719>
- [6] Fatima, I., Singh, A.B., Dhawan, P.: MASTL: A novel therapeutic target for Cancer Malignancy. *Cancer Med.* 9, 6322–6329 (2020). <https://doi.org/10.1002/cam4.3141>
- [7] Guo, K., Lu, M., Bi, J., Yao, T., Gao, J., Ren, F., Zhu, L.: Ferroptosis: mechanism, immunotherapy and role in ovarian cancer. *Front Immunol.* 15, 1410018 (2024). <https://doi.org/10.3389/fimmu.2024.1410018>
- [8] Vera, J., Lartigue, L., Vigneron, S., Gadea, G., Gire, V., Del Rio, M., Soubeyran, I., Chibon, F., Lorca, T., Castro, A.: Greatwall promotes cell transformation by hyperactivating AKT in human malignancies. *Elife.* 4, e10115 (2015). <https://doi.org/10.7554/eLife.10115>

- [9] Ocasio, C.A., Rajasekaran, M.B., Walker, S., Le Grand, D., Spencer, J., Pearl, F.M.G., Ward, S.E., Savic, V., Pearl, L.H., Hochegger, H., Oliver, A.W.: A first generation inhibitor of human Greatwall kinase, enabled by structural and functional characterisation of a minimal kinase domain construct. *Oncotarget*. 7, 71182–71197 (2016). <https://doi.org/10.18632/oncotarget.11511>
- [10] Uppada, S.B., Gowrikumar, S., Ahmad, R., Kumar, B., Szeglin, B., Chen, X., Smith, J.J., Batra, S.K., Singh, A.B., Dhawan, P.: MASTL induces Colon Cancer progression and Chemoresistance by promoting Wnt/ β -catenin signaling. *Mol Cancer*. 17, 111 (2018). <https://doi.org/10.1186/s12943-018-0848-3>
- [11] Ch, H., Hc, H., Fs, S., Pw, W., Lx, Y., Db, S., Yc, W.: An innovative NRF2 nano-modulator induces lung cancer ferroptosis and elicits an immunostimulatory tumor microenvironment. *Theranostics*. 11, (2021). <https://doi.org/10.7150/thno.57803>
- [12] Qian, B., Che, L., Du, Z.-B., Guo, N.-J., Wu, X.-M., Yang, L., Zheng, Z.-X., Gao, Y.-L., Wang, M.-Z., Chen, X.-X., Xu, L., Zhou, Z.-J., Lin, Y.-C., Lin, Z.-N.: Protein phosphatase 2A-B55 β mediated mitochondrial p-GPX4 dephosphorylation promoted sorafenib-induced ferroptosis in hepatocellular carcinoma via regulating p53 retrograde signaling. *Theranostics*. 13, 4288–4302 (2023). <https://doi.org/10.7150/thno.82132>